

Nonlinear Control Design for a Multi-Terminal VSC-HVDC System

Yijing Chen¹, Jing Dai¹, Gilney Damm², Françoise Lamnabhi-Lagarrigue¹

Abstract—This paper presents a nonlinear control strategy based on dynamic feedback linearization control theory and a backstepping-like procedure for a multi-terminal voltage-source converter based high-voltage direct current (multi-terminal VSC-HVDC) system. The controller is able to provide asymptotic stability for the power transmission system with multiple terminals. In particular, it is shown that the zero dynamics (mostly representing the DC network) is exponentially stable. These results are obtained by a stability proof for the whole system under the proposed controller, and its performance is illustrated by computer simulations.

I. INTRODUCTION

With the development of wind, solar and other renewable energy sources, there is an urgent need to integrate these decentralized and relatively small-scale power plants into the grid in an economical and environmentally friendly way. Furthermore, the increase in electricity demand requires the expansion of grid capacity. However, it is hard to upgrade the grid with overhead AC lines, which occupy large transmission line corridors. For both cases, Voltage-Source Converter based High-Voltage Direct Current (VSC-HVDC) multipoint networks could be a good solution.

At present, over 90 DC transmission projects exist in the world, the vast majority for point-to-point two-terminal HVDC transmission systems [1] and only two for multi-terminal HVDC (MTDC) systems. The traditional two-terminal HVDC transmission system can only carry out point-to-point power transfer. As the economic development and the construction of the power grid require that the DC grid can achieve power exchanges among multiple power suppliers and multiple power consumers, MTDC systems draw more and more attention. As a DC transmission network connecting more than two converter stations, the MTDC transmission system offers a larger transmission capacity than the AC network and provides a more flexible, efficient transmission method. The main applications of MTDC systems include power exchange among multi-points, connection between asynchronous networks, and integration of scattered power plants like offshore renewable energy sources such as wind farms and solar plants.

A large amount of research on two-terminal VSC-HVDC control has been carried out [2], [3], [4], [5]. In [2], an equivalent continuous-time averaged state-space model is

presented and a robust DC-bus voltage control scheme is proposed highlighting the existence of fast and slow dynamics that can be associated to the inner current control loop and outer DC-bus voltage control loop. Reference [4] proposes a control strategy under balanced and unbalanced network conditions, which contains two sets of controller: a main controller in the positive dq frame using decoupling control, and an auxiliary controller using coupling control. However, the above mentioned controllers were designed for a standard two-terminal VSC-HVDC system, not for multi-terminal VSC-HVDC system. In [6], [7], control strategies of multi-terminal VSC-HVDC systems were investigated. Reference [6] uses a droop control scheme to control the DC voltage. Reference [7] proposes a scheme for controlling and coordinating the VSC and sharing the power among the connected AC areas. However, the previously mentioned articles came from the power systems community and, as a consequence, they did not provide stability proofs.

In the present paper, a control strategy is formally designed with its mathematical stability analysis for a multi-terminal HVDC system. The controller is based on feedback linearization control theory (see [8], [9]) and it is developed by following a backstepping-like procedure (see [10], [11], [12], [13]). This controller assures asymptotic stability for the power transmission system with multiple terminals. In a second step, the behavior of the internal states of the system (known as the zero dynamics [14]), representing the transmission network, is analyzed and the zero dynamics is shown to be exponentially stable. It can then be seen that the MTDC system is asymptotically stable.

This paper is organized into five sections. In Section II, a dynamic multi-terminal VSC HVDC model is given. In Section III, a feedback control law is developed. Simulation results are presented in Section IV. Conclusions are drawn in Section V.

II. MODELING OF A MULTI-TERMINAL VSC-HVDC SYSTEM

This section introduces the state-space model of a multi-terminal VSC-HVDC system established in the synchronous dq frame, which allows for a decoupled control on the active and the reactive power, with the high-frequency pulse width modulation (PWM) characteristics of the power electronics neglected. Only the balanced condition is considered in this paper, i.e. the three phases have identical parameters and their voltages and currents have the same amplitude while phase-shifted 120° between themselves.

A converter of a multi-terminal VSC-HVDC system is shown in Fig. 1, where v_{li} is the voltage of AC area i , R_{li}

This work is supported by WINPOWER project.

¹Y. Chen, J. Dai and F. Lamnabhi-Lagarrigue are with Laboratoire des Signaux et Systèmes (LSS), Supélec, 3 rue Joliot-Curie, 91192 Gif-sur-Yvette, France (tel: +33 1 69 85 17 77, e-mail: yijing.chen@lss.supelec.fr, jing.dai@supelec.fr, francoise.lamnabhi-lagarrigue@lss.supelec.fr).

²G. Damm is with Laboratoire IBISC, Université d'Evry-Val d'Essonne, 40 rue du Pelvoux, 91020 Evry, France (e-mail: gilney.damm@ibisc.fr).

and L_{li} represent series connected phase reactors, i_{li} is the AC current through the phase reactors, v_i is the voltage on the AC side of the converter, C_i is the DC capacitor, i_{ci} and u_{ci} are the DC bus current and the DC voltage, R_{ci} and L_{ci} are the transmission cable resistance and inductance, and i_i is the current on the DC side of the converter.

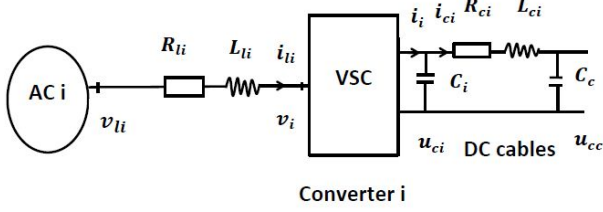


Fig. 1. One terminal in a multi-terminal VSC transmission system.

A. AC network

On the AC side of the converter station, the Kirchhoff voltage law leads to the system expressed in dq synchronous reference frame rotating at the pulsation ω_i :

$$\begin{aligned} v_{lid} - R_{li}i_{lid} - L_{li}\frac{di_{lid}}{dt} + \omega_i L_{li}i_{liq} - v_{id} &= 0 \\ v_{liq} - R_{li}i_{liq} - L_{li}\frac{di_{liq}}{dt} - \omega_i L_{li}i_{lid} - v_{iq} &= 0 \end{aligned}$$

By using PWM technology, the amplitude of the converter output voltage v_{id} and v_{iq} are controlled by the modulation index M_{di} and M_{qi} as:

$$\begin{aligned} v_{id} &= \frac{M_{di}}{2} u_{ci} \\ v_{iq} &= \frac{M_{qi}}{2} u_{ci} \end{aligned}$$

By neglecting the resistance of the converter reactor and switching losses, the instantaneous active power and the reactive power on the AC side of the converters can be expressed as:

$$P_{li} = \frac{3}{2}(v_{lid}i_{lid} + v_{liq}i_{liq}) \quad (1)$$

$$Q_{li} = \frac{3}{2}(v_{liq}i_{lid} - v_{lid}i_{liq}) \quad (2)$$

B. DC line

By applying the Kirchhoff voltage and current laws to the DC circuit, the DC side of the converter is modeled by:

$$\begin{aligned} \frac{du_{ci}}{dt} &= -\frac{1}{C_i}i_{ci} + \frac{1}{C_i}i_i \\ \frac{di_{ci}}{dt} &= \frac{1}{L_{ci}}u_{ci} - \frac{R_{ci}}{L_{ci}}i_{ci} - \frac{1}{L_{ci}}u_{cc} \end{aligned}$$

C. AC-DC power coupling

Because of the active power balance on both sides of the converter, we have $u_{ci}i_i = v_{iA}i_{liA} + v_{iB}i_{liB} + v_{iC}i_{liC}$. Thus, i_i can be expressed as:

$$i_i = \frac{3}{4}(M_{di}i_{lid} + M_{qi}i_{liq})$$

A radial structure is chosen for the interconnection of the N terminals, as shown in Fig. 2, which is represented as:

$$\frac{du_{cc}}{dt} = \frac{1}{C_c} \sum_{k=1}^N i_{ck}$$

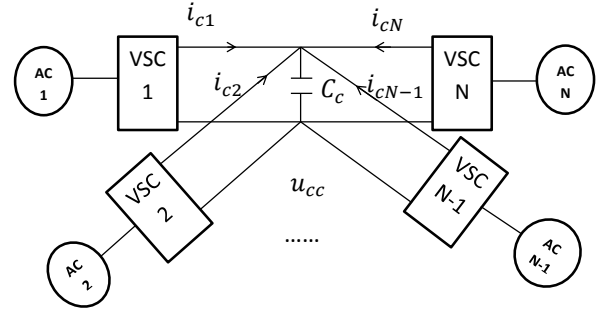


Fig. 2. The interconnection between N terminals.

D. Global model

The full state-space model of the N -terminal VSC-HVDC system is written as:

$$\begin{cases} \frac{di_{lid}}{dt} = -\frac{R_{li}}{L_{li}}i_{lid} + \omega_i i_{liq} - \frac{1}{L_{li}}M_{di}\frac{u_{ci}}{2} + \frac{1}{L_{li}}v_{lid} \\ \frac{di_{liq}}{dt} = -\frac{R_{li}}{L_{li}}i_{liq} - \omega_i i_{lid} - \frac{1}{L_{li}}M_{qi}\frac{u_{ci}}{2} + \frac{1}{L_{li}}v_{liq} \\ \frac{du_{ci}}{dt} = -\frac{1}{C_i}i_{ci} + \frac{1}{C_i}\frac{3}{4}(M_{di}i_{lid} + M_{qi}i_{liq}) \\ \frac{di_{ci}}{dt} = \frac{1}{L_{ci}}u_{ci} - \frac{R_{ci}}{L_{ci}}i_{ci} - \frac{1}{L_{ci}}u_{cc} \\ \frac{du_{cc}}{dt} = \frac{1}{C_c}(\sum_{k=1}^N i_{ck}) \end{cases} \quad (3)$$

where $i = 1, \dots, N$.

The global state-space model is summarized as:

- State variables: $i_{lid}, i_{liq}, u_{ci}, i_{ci}, u_{cc}$.
- Control variables: M_{di}, M_{qi} .
- External signals: v_{lid}, v_{liq} .
- The dimension of the system (3) is $4N + 1$.

III. CONTROL SCHEME

In this section, we present the detailed synthesis of the controller for one converter. The control objective is to make the converter's DC voltage u_{ci} and the reactive power Q_{li} track their reference values u_{ci}^* and Q_{li}^* . We use a backstepping-like procedure to design such a controller.

A. Controller synthesis

1) *First step*: The first step of the backstepping-like procedure consists in making the AC currents i_{lid} and i_{liq} follow their reference trajectories i_{lid}^* and i_{liq}^* (yet to be designed in a second step), i.e. to eliminate the dq current errors \tilde{i}_{lid} and \tilde{i}_{liq} where $\tilde{i}_{lid} = i_{lid} - i_{lid}^*$ and $\tilde{i}_{liq} = i_{liq} - i_{liq}^*$.

Following a feedback linearization procedure, we design the control laws as

$$\begin{cases} u_{id} = \frac{di_{lid}}{dt} = \frac{d\tilde{i}_{lid}}{dt} + \frac{di_{lid}^*}{dt} \\ u_{iq} = \frac{di_{liq}}{dt} = \frac{d\tilde{i}_{liq}}{dt} + \frac{di_{liq}^*}{dt} \end{cases} \quad (4)$$

where u_{id} and u_{iq} are auxiliary inputs, which control independently i_{lid} and i_{liq} . By substituting (4) into the dq current equations of the system (3), the control variables M_{di} and M_{qi} are expressed as:

$$\begin{cases} M_{di} = \frac{2L_{li}}{u_{ci}} \left(-\frac{R_{li}}{L_{li}} i_{lid} + \omega_i i_{liq} + \frac{1}{L_{li}} v_{lid} - u_{id} \right) \\ M_{qi} = \frac{2L_{li}}{u_{ci}} \left(-\frac{R_{li}}{L_{li}} i_{liq} - \omega_i i_{lid} + \frac{1}{L_{li}} v_{liq} - u_{iq} \right) \end{cases} \quad (5)$$

To assure that the errors \tilde{i}_{lid} and \tilde{i}_{liq} will converge to zero, the following augmented states are proposed:

$$\begin{cases} \dot{\varphi}_{id} = \tilde{i}_{lid} \\ \dot{\tilde{i}}_{lid} = -k_{id}\tilde{i}_{lid} - \lambda_{id}\varphi_{id} \end{cases} \quad (6)$$

$$\begin{cases} \dot{\varphi}_{iq} = \tilde{i}_{liq} \\ \dot{\tilde{i}}_{liq} = -k_{iq}\tilde{i}_{liq} - \lambda_{iq}\varphi_{iq} \end{cases} \quad (7)$$

where k_{id} , k_{iq} , λ_{id} and λ_{iq} are positive constants. By combining (4), (6) and (7), we have:

$$\begin{cases} u_{id} = -k_{id}\tilde{i}_{lid} - \lambda_{id}\varphi_{id} + \frac{di_{lid}^*}{dt} \\ u_{iq} = -k_{iq}\tilde{i}_{liq} - \lambda_{iq}\varphi_{iq} + \frac{di_{liq}^*}{dt} \end{cases} \quad (8)$$

2) *Second step:* The second step of the backstepping-like procedure determines the dq current reference values so that the converter tracks the reference values for the DC voltage and the reactive power.

By assuming a dq frame orientation such that $v_{liq} = 0$, i_{liq}^* can be obtained directly from the reactive power's reference:

$$i_{liq}^* = -\frac{2Q_{li}^*}{3v_{lid}} \quad (9)$$

As to i_{lid}^* , it is used to keep the DC voltage constant at its reference point u_{ci}^* . i_{lid}^* is calculated by the DC voltage controller as follows. By substituting (5) into the third equation of (3), we have:

$$\begin{aligned} \dot{u}_{ci} = & -\frac{1}{C_i} i_{ci} + \frac{3}{2} \frac{1}{C_i u_{ci}} [i_{lid}(-R_{li}i_{lid} + v_{lid} - L_{li}u_{id}) \\ & + i_{liq}(-R_{li}i_{liq} + v_{liq} - L_{li}u_{iq})] \end{aligned} \quad (10)$$

Then, by substituting (8) into (10), the DC voltage dynamics is given by:

$$\begin{aligned} \dot{u}_{ci} = & -\frac{1}{C_i} i_{ci} + \frac{3}{2} \frac{1}{C_i u_{ci}} [i_{lid}(-R_{li}i_{lid} + v_{lid} + L_{li}k_{id}\tilde{i}_{lid} \\ & + L_{li}\lambda_{id}\varphi_{id} - L_{li}\frac{di_{lid}^*}{dt}) + i_{liq}(-R_{li}i_{liq} + v_{liq} \\ & + L_{li}k_{iq}\tilde{i}_{liq} + L_{li}\lambda_{iq}\varphi_{iq} - L_{li}\frac{di_{liq}^*}{dt})] \end{aligned} \quad (11)$$

To maintain the DC voltage u_{ci} at its set value, the desired dynamics of voltage error \tilde{u}_{ci} is expressed as:

$$\begin{aligned} \dot{\varphi}_{ci} &= \tilde{u}_{ci} \\ \dot{\tilde{u}}_{ci} &= -k_{ci}\tilde{u}_{ci} - \lambda_{ci}\varphi_{ci} \end{aligned} \quad (12)$$

where $\tilde{u}_{ci} = u_{ci} - u_{ci}^*$. The above equation can also be written as:

$$\dot{u}_{ci} = -k_{ci}\tilde{u}_{ci} - \lambda_{ci}\varphi_{ci} + \dot{u}_{ci}^* \quad (13)$$

Since the desired values for u_{ci}^* , Q_{li}^* are constant, $\frac{du_{ci}^*}{dt}$ and $\frac{di_{liq}^*}{dt}$ are zero.

By combining (11) and (13), $\frac{di_{lid}^*}{dt}$ is deduced as:

$$\begin{aligned} \frac{di_{lid}^*}{dt} = & -\frac{2}{3} \frac{u_{ci}}{i_{lid}} \frac{C_i}{L_{li}} (-k_{ci}\tilde{u}_{ci} - \lambda_{ci}\varphi_{ci} + \frac{i_{ci}}{C_i}) + \frac{u_{ci}}{2L_{li}} \frac{i_{liq}}{i_{lid}} M_{qi} \\ & + (-\frac{R_{li}}{L_{li}} i_{lid} + \omega_i i_{liq} + \frac{v_{lid}}{L_{li}} + k_{id}\tilde{i}_{lid} + \lambda_{id}\varphi_{id}) \end{aligned} \quad (14)$$

B. Stability study

Theorem 1: Under the control laws (5), (6), (7), (9), (12) and (14), the multi-terminal VSC-HVDC system described by (3) is asymptotically stabilized to their reference values u_{ci}^* and Q_{li}^* . Furthermore, this result is independent of the network parameters L_{ci} , R_{ci} , C_{ci} .

Proof: In the considered case, all the N converters control their DC voltages. Since it is desired to keep u_{ci} , i_{lid} and i_{liq} at their reference values u_{ci}^* , i_{lid}^* and i_{liq}^* , we define the outputs of the system as:

$$y = [u_{ci} \ i_{lid} \ i_{liq}]^T$$

To simplify our analysis, we first shift the reference values of the whole system to the origins by introducing the following state variables:

$$\tilde{x} = [\tilde{i}_{lid} \ \tilde{i}_{liq} \ \tilde{u}_{ci} \ \tilde{i}_{ci} \ \tilde{u}_{cc}]^T$$

where $\tilde{i}_{ci} = i_{ci} - i_{ci}^*$, $\tilde{u}_{cc} = u_{cc} - u_{cc}^*$, and i_{ci}^* and u_{cc}^* are the equilibrium values of i_{ci} and u_{cc} . The new output error variables are defined as:

$$\tilde{y} = [\tilde{u}_{ci} \ \tilde{i}_{lid} \ \tilde{i}_{liq}]^T$$

The system (3) can be expressed in terms of the new variables as:

$$\begin{cases} \frac{d\tilde{i}_{lid}}{dt} = -\frac{R_{li}\tilde{i}_{lid}}{L_{li}} + \omega_i\tilde{i}_{liq} - \frac{1}{2L_{li}}(M_{di}u_{ci} - M_{di}^*u_{ci}^*) \\ \frac{d\tilde{i}_{liq}}{dt} = -\frac{R_{li}\tilde{i}_{liq}}{L_{li}} - \omega_i\tilde{i}_{lid} - \frac{1}{2L_{li}}(M_{qi}u_{ci} - M_{qi}^*u_{ci}^*) \\ \frac{d\tilde{u}_{ci}}{dt} = -\frac{1}{C_i}\tilde{i}_{ci} \\ \quad + \frac{1}{C_i}\frac{3}{4}(M_{di}i_{lid} - M_{di}^*i_{lid}^* + M_{qi}i_{liq} - M_{qi}^*i_{liq}^*) \\ \frac{d\tilde{i}_{ci}}{dt} = \frac{1}{L_{ci}}\tilde{u}_{ci} - \frac{R_{ci}\tilde{i}_{ci}}{L_{ci}} - \frac{1}{L_{ci}}\tilde{u}_{cc} \\ \frac{d\tilde{u}_{cc}}{dt} = \frac{1}{C_c}(\sum_{k=1}^N \tilde{i}_{ck}) \end{cases} \quad (15)$$

where $i = 1, \dots, N$ and M_{di}^* and M_{qi}^* are the equilibrium values of M_{di} and M_{qi} .

In order to analyze the stability of the new system (15), we divide the state variables \tilde{x} into two parts:

$$\begin{aligned}\eta &= [\tilde{i}_{ci} \ \tilde{u}_{cc}]^T \\ \xi &= [\tilde{i}_{lid} \ \tilde{i}_{liq} \ \tilde{u}_{ci}]^T\end{aligned}$$

Then, system (15) can be considered as in the normal form:

$$\begin{cases} \dot{\eta} = f_1(\eta, \xi) \\ \dot{\xi} = f_2(\eta, \xi, u) \end{cases} \quad (16)$$

with

$$u = f_3(\eta, \xi) \quad (17)$$

where $u = [M_{di} \ M_{qi}]$.

We see that if the output is identically zero, i.e. $y \equiv 0$, then $\xi \equiv 0$, and the behavior of the system (16) is governed by the differential equation:

$$\dot{\eta} = f_1(\eta, 0) \quad (18)$$

which is called the zero dynamics of the system.

We now study the behavior of η and ξ . By combining (5) (6) (7) and (12), the closed-loop error system can be written as:

$$\dot{\zeta} = A\zeta$$

where $\zeta = [\varphi_{id} \ \tilde{i}_{lid} \ \varphi_{iq} \ \tilde{i}_{liq} \ \varphi_{ci} \ \tilde{u}_{ci}]^T$ and $A = \text{diag}(A_{id}, A_{iq}, A_{ci})$ with

$$\begin{aligned}A_{id} &= \begin{pmatrix} 0 & 1 \\ -\lambda_{id} & -k_{id} \end{pmatrix} \\ A_{iq} &= \begin{pmatrix} 0 & 1 \\ -\lambda_{iq} & -k_{iq} \end{pmatrix} \\ A_{ci} &= \begin{pmatrix} 0 & 1 \\ -\lambda_{ci} & -k_{ci} \end{pmatrix}\end{aligned}$$

It is easy to verify that matrix A is Hurwitz. Thus, ζ (hence ξ) is exponentially stable under the proposed control law. It remains now to study the behavior of the state variables η as ξ converges to zero. In fact, when $\xi = 0$, η is governed by the following differential equation:

$$\begin{bmatrix} \dot{\tilde{i}}_{c1} & \dot{\tilde{i}}_{c2} & \dots & \dot{\tilde{i}}_{cN} & \dot{\tilde{u}}_{cc} \end{bmatrix}^T = B \begin{bmatrix} \tilde{i}_{c1} & \tilde{i}_{c2} & \dots & \tilde{i}_{cN} & \tilde{u}_{cc} \end{bmatrix}^T$$

$$\text{where } B = \begin{bmatrix} -\frac{R_{c1}}{L_{c1}} & 0 & \dots & 0 & -\frac{1}{L_{c1}} \\ 0 & -\frac{R_{c2}}{L_{c2}} & \dots & 0 & -\frac{1}{L_{c2}} \\ \vdots & \vdots & \ddots & \vdots & \vdots \\ \frac{1}{C_c} & \frac{1}{C_c} & \dots & \frac{1}{C_c} & 0 \end{bmatrix}.$$

Thus, the zero dynamics of the system (15) is:

$$f_1(\eta, 0) = B\eta \quad (19)$$

To investigate the stability of (19), a Lyapunov function V is chosen as:

$$V = \sum_{k=1}^N \frac{L_{ck}}{C_c} \tilde{i}_{ck}^2 + \tilde{u}_{cc}^2 \quad (20)$$

The derivative of V along the trajectories of (19) is given by:

$$\begin{aligned}\dot{V} &= \sum_{k=1}^N \frac{L_{ck}}{C_c} \tilde{i}_{ck} \dot{\tilde{i}}_{ck} + \tilde{u}_{cc} \dot{\tilde{u}}_{cc} \\ &= \sum_{k=1}^N \frac{L_{ck}}{C_c} \tilde{i}_{ck} \left(-\frac{R_{ck}}{L_{ck}} \tilde{i}_{ck} - \frac{1}{L_{ck}} \tilde{u}_{cc} \right) + \tilde{u}_{cc} \frac{1}{C_c} \left(\sum_{k=1}^N \tilde{i}_{ck} \right) \\ &= -\sum_{k=1}^N \frac{R_{ck}}{C_c} \tilde{i}_{ck}^2 \leq 0\end{aligned} \quad (21)$$

\dot{V} is negative semidefinite. To find $S = \{\eta \in \mathbb{R}^{N+1} | \dot{V}(\eta) = 0\}$, note that

$$\dot{V}(\eta) = 0 \Rightarrow \tilde{i}_{ck} = 0, \quad k = 1, \dots, N \quad (22)$$

Hence, $S = \{\eta \in \mathbb{R}^{N+1} | \tilde{i}_{ck} = 0, \quad k = 1, \dots, N\}$. Let η be a solution that belongs identically to S :

$$\tilde{i}_{ck} \equiv 0 \Rightarrow \dot{\tilde{i}}_{ck} \equiv 0 \Rightarrow \tilde{u}_{cc} \equiv 0 \quad (23)$$

Therefore, the only solution that can stay identically in S is the trivial solution $\eta \equiv 0$. Thus, according to LaSalle's theorem and its corollary, the zero dynamics of the system (15) is asymptotically stable.

Therefore, the whole system (15) is asymptotically stabilized at $(\eta, \xi) = (0, 0)$ under the proposed controller. ■

IV. SIMULATION RESULTS

The proposed controller is tested by computer simulations on a three-terminal VSC-HVDC system shown in Fig. 3. All three VSC converters operate in DC voltage control mode. The terminal parameter values are given in Table I. We choose $\omega_i = 314$, and $v_{li} = 230$ kV. The feedback control gains are chosen as $k_{id} = 100$, $\lambda_{id} = 100$, $k_{iq} = 100$, $\lambda_{iq} = 100$, $k_{ci} = 25$, $\lambda_{ci} = 5$. The sequence of events listed in Table II is applied to the system. In addition, Q_{l1} , Q_{l2} and Q_{l3} are set to zero to have a unitary power factor, which means that i_{l2q}^* , i_{l2q}^* and i_{l3q}^* are zero.

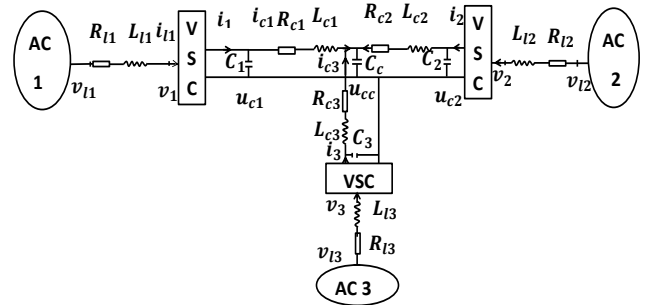


Fig. 3. A three-terminal VSC-HVDC transmission system.

Simulation results are shown in Figs. 4-9. The regulation response of each converter's DC voltage is illustrated in Figs. 4, 6, and 8 where the black curve represents the DC voltage's reference value and the red one is the response. At the start

Terminal	R_{li}	L_{li}	R_{ci}	L_{ci}	C_i
1	13.79 Ω	31.02 mH	0.2085 Ω	2.4 mH	12 μ F
2	12.79 Ω	33.02 mH	0.2 Ω	1 mH	12 μ F
3	13.57 Ω	40.02 mH	0.235 Ω	3.5 mH	12 μ F

TABLE I
PARAMETER VALUES OF THE TERMINALS.

Time (s)	Event
0	$u_{c1}^* = 101$ kV, $u_{c2}^* = 100$ kV, $u_{c3}^* = 99.8$ kV
1	$u_{c1}^* = 101.2$ kV, $u_{c2}^* = 101$ kV, $u_{c3}^* = 99.9$ kV
4	$u_{c1}^* = 102.2$ kV
5	$u_{c2}^* = 102.0$ kV
6	$u_{c3}^* = 100.9$ kV

TABLE II
SEQUENCE OF EVENTS APPLIED TO THE SYSTEM.

of the simulation, the converter work at their initial reference DC voltage. After a step change in each DC voltage reference value at $t = 1$ s, the actual u_{ci} reaches the new u_{ci}^* before $t = 2$ s, as shown in Figs. 4, 6, and 8. At $t = 4$ s, only u_{c1}^* has a step change, which u_{c1} follows before $t = 5$ s, as can be seen in Fig. 4. From $t = 4$ s to $t = 5$ s, u_{c2} and u_{c3} keep unchanged and remain at their reference values, as shown in Figs. 6 and 8. After u_{c2} and u_{c3} have their reference values reset respectively at $t = 5$ s and $t = 6$ s, they attain their new reference values and have no effect on u_{c1} .

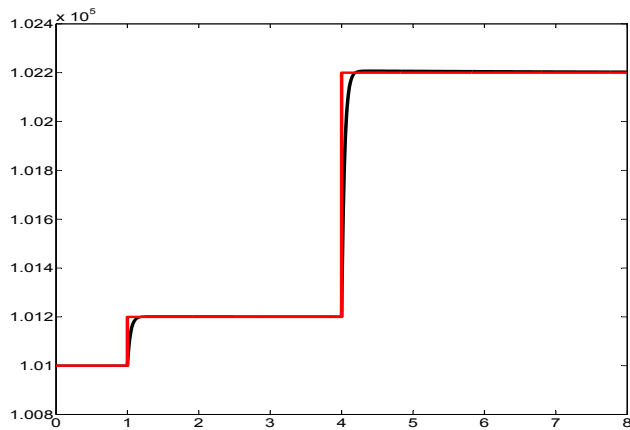


Fig. 4. u_{c1} response.

Figs. 5, 7 and 9 illustrate each converter's DC current i_{ci} . We see that, once the DC voltage reference value is changed, the DC current is also changed and reaches the new reference point. This shows the effectiveness of the DC voltage controller. A negative i_{ci} means that AC area i absorbs active power from the DC grid, while a positive i_{ci} means that AC area i injects active power into DC grid.

Simulation results (figures not shown here) show that the converter quadrature current i_{liq} is always very close to zero no matter how we change the DC voltage reference value. The reason is that the quadrature current is controlled by the reactive controller, which keeps i_{liq} close to zero in order to have a zero Q_{li} .

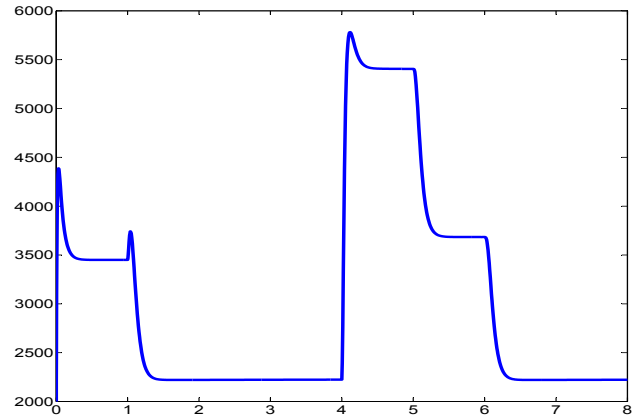


Fig. 5. i_{c1} response.

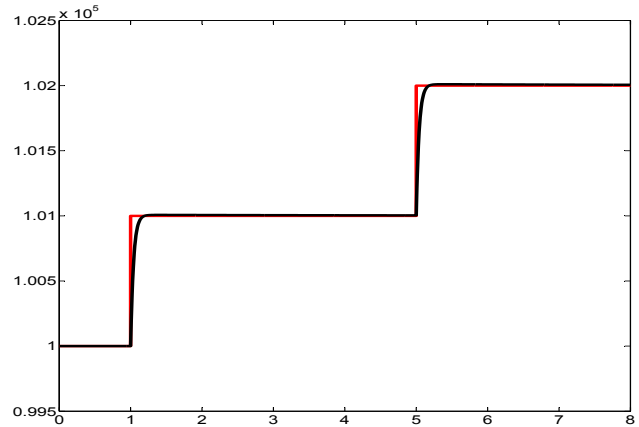


Fig. 6. u_{c2} response.

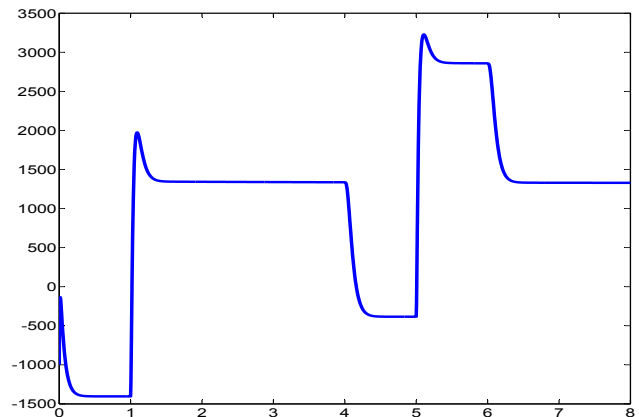


Fig. 7. i_{c2} response.

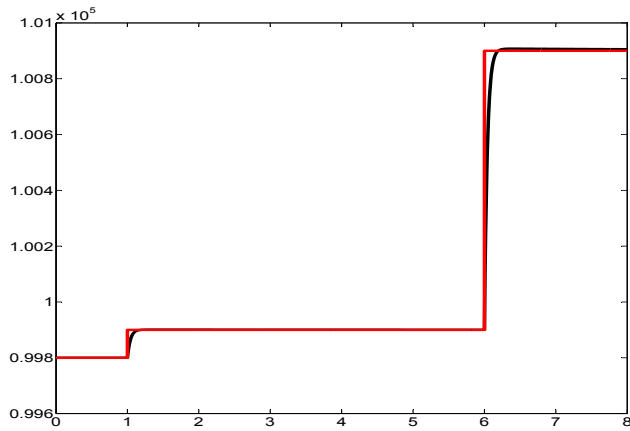


Fig. 8. u_{c3} response.

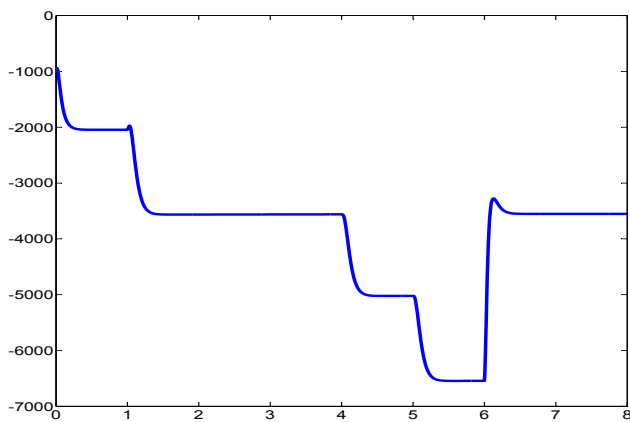


Fig. 9. i_{c3} response.

V. CONCLUSIONS

In this paper, a nonlinear controller is designed for a multi-terminal VSC-HVDC system. The proposed control law is based on dynamic feedback linearization strategy and a backstepping-like procedure. A detailed stability analysis by means of the zero dynamics approach for the nonlinear system shows that the MTDC system is asymptotically stable independently of network parameters. Simulation results show that the proposed control strategy is able to regulate the DC-bus voltage with good dynamic performance.

REFERENCES

- [1] P. Kundur, *Power System Stability and Control*. McGraw-Hill, 1994.
- [2] J. L. Thomas, S. Poullain, and A. Benchaib, "Analysis of a robust DC-bus voltage control system for a VSC transmission scheme," in *Seventh International Conference on AC and DC Transmission*, (London), November 2001.
- [3] M. Rashed, S. El-Anwar, and F. Youssef, "Nonlinear control scheme for VSC-HVDC transmission systems," in *12th International Middle-East Power System Conference, MEPCON 2008*, pp. 486–491, March 2008.
- [4] L. Xu and B. R. Andersen, "Control of VSC transmission systems under unbalanced network conditions," *IEEE PES Transmission and Distribution Conference and Exposition*, vol. 2, pp. 626–632, 2003.

- [5] L. Xu, B. Andersen, and P. Cartwright, "VSC transmission operating under unbalanced AC conditions - analysis and control design," *IEEE Transactions on Power Delivery*, vol. 20, pp. 427–434, January 2005.
- [6] O. Gomis-Bellmunt, A. Egea-Alvarez, A. Junyent-Ferre, J. Liang, J. Ekanayake, and N. Jenkins, "Multiterminal HVDC-VSC for offshore wind power integration," in *IEEE Power and Energy Society General Meeting*, pp. 1–6, July 2011.
- [7] L. Xu, B. Williams, and L. Yao, "Multi-terminal DC transmission systems for connecting large offshore wind farms," in *IEEE Power and Energy Society General Meeting - Conversion and Delivery of Electrical Energy in the 21st Century*, pp. 1–7, July 2008.
- [8] H. Khalil, *Nonlinear Systems*. New Jersey: Prentice Hall, 3rd ed., 1996.
- [9] R. Marino and P. Tomei, *Nonlinear Control Design - Geometric, Adaptive and Robust*. Hemel Hempstead, London: Prentice Hall, 1995.
- [10] C. Verrelli and G. Damm, "Adaptive robust transient stabilization problem for a synchronous generator in a power network," *International Journal Control (full paper)*, vol. 83, no. 4, pp. 816–828, April 2010.
- [11] G. Damm, F. Lamnabhi-Lagarrigue, and R. Marino, "Adaptive nonlinear excitation control of synchronous generators with unknown mechanical power," in *Proc. 1st IFAC Symposium on System Structure and Control*, (Prague-Czech Republic), IFAC, August 2001.
- [12] G. Damm, F. Lamnabhi-Lagarrigue, R. Marino, and C. Verrelli, *Transient Stabilization and Voltage Regulation of a Synchronous Generator*. ISTE-Taming Heterogeneity and Complexity of Embedded Control, 2006.
- [13] S. Bregeon, A. Benchaib, S. Poullain, and J. L. Thomas, "Robust DC bus voltage control based on backstepping and lyapunov methods for long distance VSC transmission scheme," in *EPE*, (Toulouse), September 2003.
- [14] A. Isidori, *Nonlinear Control Systems, Third Edition*. Springer, 1995.